PROGRESS IN COLOR, COLORANTS AND COATINGS

available online @ www.pccc.icrc.ac.ir

Prog. Color Colorants Coat. 12 (2019), 203-209

Ministry of Science, Research and Technology
Institute for Color Science and Technology

Influence of Ni Deposition and Subsequent N^+ Ion Implantation at Different Implantation Energies on Nano-Structure and Corrosion Behavior of 316 Stainless Steels

A. Grayeli Korpi[1*], S. Rezaee[2], P. Balashabadi[1]

[1.] Physics and Accelerators Research School, Nuclear Science & Technology Research Institute (NSTRI), P. O. Box: 11365-3486, Tehran, Iran

[2.] Department of Physics, Kermanshah Branch, Islamic Azad University, P. O. Box: 671791-7855, Kermanshah, Iran.

ARTICLE INFO

Article history:
Received: 3 Dec 2018
Final Revised: 25 Feb 2019
Accepted: 26 Feb 2019
Available online: 25 Jun 2019

Keywords:
Ni thin films
Corrosion
Potentiodynamic
Stainless steel
SEM.

ABSTRACT

Nickel films of 300 nm thickness were deposited by electron beam evaporation at room temperature on 316 stainless steels. Corrosion studies of Ni coated 316 SS have been performed after N^+ ion implantation at different energies of 20, 40, 60 and 80 keV. The structure and surface morphology of the films were evaluated using X-ray diffraction (XRD), atomic force microscope (AFM) and scanning electron microscope (SEM). X-ray diffraction (XRD) analysis showed formation of nickel nitride phases. The corrosion behavior of the samples was evaluated by potentiodynamic polarization test in 3.5% NaCl solution. The subsequent Tafel analysis revealed nobler open circuit potential and lower corrosion current density values with increase of beam energy. By increasing the implantation energy, diffusion effect enhances, hence, larger grains with smoother surfaces are formed. The smoother surfaces show higher resistance in the corroding medium. Increase in implantation energy was beneficial in improving the corrosion resistance. Prog. Color Colorants Coat. 12 (2019), 203-209© Institute for Color Science and Technology.

1. Introduction

Stainless steels (SS) are defined as iron-based alloys containing at least 10.5% chromium and a maximum of 1.2% carbon. They are employed for a variety of applications in both industrial and domestic environments. Typical areas of use include piping systems, heat exchangers, tanks and process vessels for food, chemical, pharmaceutical, pulp and paper, and other industrial processes [1-4].

316 stainless steel is molybdenum-bearing austenitic stainless steel. The higher nickel and molybdenum contents in this grade allow it to demonstrate better overall corrosion resistant properties, especially with regard to pitting and crevice corrosion in chloride environments. Common uses for 316 stainless steel are in construction of exhaust manifolds, furnace parts, heat exchangers, jet engine parts, pharmaceutical and photographic equipments, valve and pump parts, chemical processing equipments, tanks and evaporators [5, 6].

Several approaches including coatings, ion implantation and corrosion inhibitors have been employed to modify corrosion protection [7-9]. One of the most useful techniques to modify surface layers of

*Corresponding author: grayli@ut.ac.ir

materials is the ion implantation. The interaction between ion beams and target leads to the improvement of corrosion resistance, hardness, wear resistance and high temperature oxidation resistance. This method can yield desirable surface properties such as corrosion resistance while the physical and mechanical stability of the bulk materials is not compromised [10-15]. Any element can be introduced into the surface of the substrate in selected depths and concentrations by ion implantation.

For many applications, nitrogen ions are used to improve the mechanical properties of stainless steels. Among several species, nitrogen is also used extensively to improve surface hardness and corrosion resistance of materials. Nitrogen is a very strong austenite structure former which substantially increases the mechanical strength of steel and enhances its resistance to localized corrosion. Many studies on nitrogen implantation into metals have shown the increased corrosion resistance. Improved corrosion properties are usually attributed to the nitride formation and hardness enhancement because of the implanted ions [16-21].

In this paper, the aim is to produce surface modified layer on commercial 316 stainless steels by nickel deposition and nitrogen implantation. In this type of deposition, the main advantage of N^+ implantation technique is the existence of a surface-modified region enriched with alloying elements that possesses hardness, corrosion resistance and wear resistance. In this work, the effects of ion implantation energy have been studied on the corrosion resistance of N^+ implanted and Ni coated austenitic 316 stainless steels which demonstrate applications in chemical, petrochemical and power generation industries as well as in human body surgical implants in 3.5 % NaCl solution.

2. Experimental

Two systems consisted of electron gun and ion source have been used to implant N^+ in nickel layers so that they were first placed under the 18×18mm stainless steel 316 layers inside the chamber at a distance of 50cm above the evaporation set. Then, the Edwards E19 A3 deposition system was used with rotary and diffusion pumps up to a pressure of 2×10^{-6} mbar, and the deposition action is performed at a rate of 1.0Å/s at the room temperature from the nickel target with a purity of 99.98%. Then, a Kaufman ion source with a multi-CUSP magnetic field consisting of a tungsten heat cathode was employed for N^+ implanting in layers in which filament causes electron emission due to the applied voltage. After that, the electrons ionize the (nitrogen) gas in the compartment on their path toward the anode to compose plasma with a certain density. The ions exit the plasma by a strong electric field derived from a system of multi-hole electrodes to focus in a beam and bombard the nickel layers at a gas pressure of 3×10^{-5}mbar. In this regard, the existing gas ions were placed in the nickel layers with a substrate temperature of 400K. In addition, in order to investigate the physical and electrical properties of the layers, all of the parameters are kept constant and only the effect of different radiation energies from the ion source has been investigated (Table 1).

Table 1: The condition of implantation, average and Rms surface roughness, crystallite size and corrosion parameters.

Sample		Energy (keV)	R_{ave} (nm)	Rms (nm)	D_{XRD} (nm)	Corrosion current density (μA cm^{-2})	Corrosion potential (V vs. SCE)
316 SS		-	-	-	-	74.13	-0.43
Implanted samples	1	20	76.6	91.4	28.8	8.01	-0.35
	2	40	66.2	82.6	33.4	1.47	-0.23
	3	60	30.1	35.6	71.1	1.23	-0.20
	4	80	20.1	22.8	99.3	0.14	-0.15

Crystallography of the films was evaluated using a Siemens D500 X-ray Diffractometer (Cu Ka radiation; 40kV, 30mA) with a step size of 0.02° and count time of 1s per step. The atomic force microscopy was used in non-contact mode to study the surface morphology of the fabricated nanostructure thin films. Using the Nova and jmicro vision software, the average and root mean square are extracted from the AFM analyses. All images were obtained over an area of 1 μm×1 μm.

Electrochemical measurements were carried out in a conventional three-electrode cell using a computer-assisted potentiostat (273A, EG & G). A saturated calomel electrode and a platinum electrode were used as reference and auxiliary electrodes, respectively. The test sample was mounted in a fixture acted as the working electrode. Potentiodynamic polarization measurements were performed by sweeping the potential from -400OCP and preceded in the positive direction with a scan rate of 1 mV/s. The test solution was 3.5% NaCl, prepared from reagent grade NaCl and distilled water. The samples were mounted in a test fixture to offer an exposed surface area of 1.0cm^2. Before starting the test, the samples were immersed in the solution for 20 min so that the open circuit potential was stabilised.

Morphology and surface appearance of samples were analyzed after corrosion test by scanning electron microscope (SEM: LEO 440i).

3. Results and Discussion

3.1. XRD

The XRD patterns of the nickel deposited and N^+ implanted 316 SS at implantation energies of 20, 40, 60 and 80keV, as well as that of uncoated 316 SS are presented in Figure 1. The XRD pattern of the uncoated sample shows the presence of austenite peaks at 2θ=43.7°, 50.7°, 74.8° and 90.0° corresponding to γ–Fe(111), γ–Fe(200), γ–Fe(220) and γ–Fe(311), respectively.

In addition to the austenite peaks, the diffraction peaks in N^+ implanted samples mainly show nickel nitride and nickel diffraction lines. The XRD pattern of the sample implanted at 20 keV reveals a nickel nitride peak at 2θ=44.48º corresponding to Ni_3N(111) line and the peak of Ni(200) at 2θ=51.85º. With increasing the implantation energy to 40 keV, the intensity of nickel nitride peak increased while the intensity of Ni(200) decreased. When implantation energy is increased to 60 keV, a peak at 2θ=33.78º belonging to Ni_4N(110) can be observed, in addition to Ni_3N(111) and Ni(200) lines. At higher implantation energy of 80 keV, nitride peaks, namely Ni_4N(110) and Ni_3N(111) are intensified while Ni(200) peak is vanished.

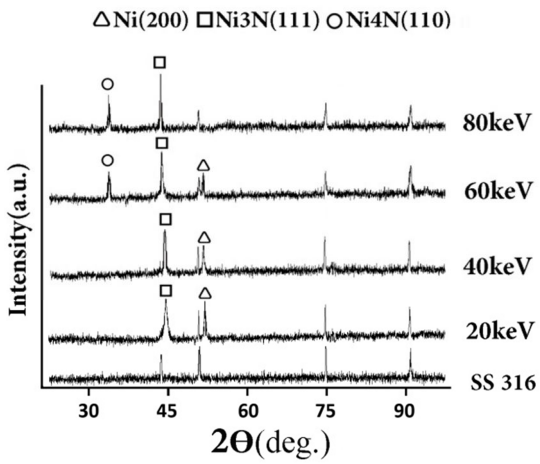

Figure 1: XRD patterns of 316 Stainless Steel and nickel coated and implanted samples with different implantation energy.

The crystallite size, D (coherently diffracting domains), is obtained using the Scherrer formula (Eq. 1) [22]:

$$D = \frac{k\lambda}{B\cos\theta} \quad (1)$$

where λ is the wavelength of X-ray, θ is Bragg angle, k is a dimensionless constant which is related to the shape and distribution of crystallites [22]. It can be included a correction for instrumental broadening in this calculation, which is usually known as full width half maximum (FWHM) measurement technique (Eq. 2):

$$B = \sqrt{W_0^2 - W_i^2} \quad (2)$$

where W_0 and W_i are FWHMs of the sample and the stress free sample (annealed powder sample), respectively. The crystal size variation with implantation energy obtained from $Ni_3N(111)$ line is given in Table 1. The general trend is an increase with implantation energy.

3.2. AFM

The surface morphology of N^+ ion implanted samples was examined by AFM and the effects of implantation energy are studied. The surface morphology images of samples are shown in Figure 2. The surface roughness of the samples is given in Table 1.

Figure 2(a) is the AFM image of N^+ implanted sample at 20 keV. Column-like grains are being to form on the surface. Surface morphology of other implanted samples at higher implantation energies is shown in Figure 2(b-d). By increasing the implantation energy, larger grains are formed which is due to the enhanced surface diffusion effect at higher temperatures. Finally, at the highest implantation energy, 80keV, the sample surface is covered with homogenous grains. Here, the surface diffusion and the implantation process as well as the gettering effect have influenced the formation of different composites of nickel nitride.

3.3. Polarization

Figure 3 shows potentiodynamic polarization curves of the uncoated N^+ implanted and Ni coated 316 SS at different energies in 3.5% NaCl solution. The polarization tests demonstrate improvement in corrosion resistance with increase in implantation energy. The quantitative values of corrosion related parameters obtained from the polarization plots are given in Table 1. These results show that by increasing the implantation energy, the corrosion current density decreases and the corrosion potential increases. It can be seen from Table 1 that the highest value for corrosion potential, -0.15V, and the lowest corrosion current density, 0.14μAcm^{-2}, are belong to sample implanted at 80 keV. The comparison of polarization results shows significant effect of N^+ ion implantation on the enhancement of corrosion inhibition of 316 stainless steel.

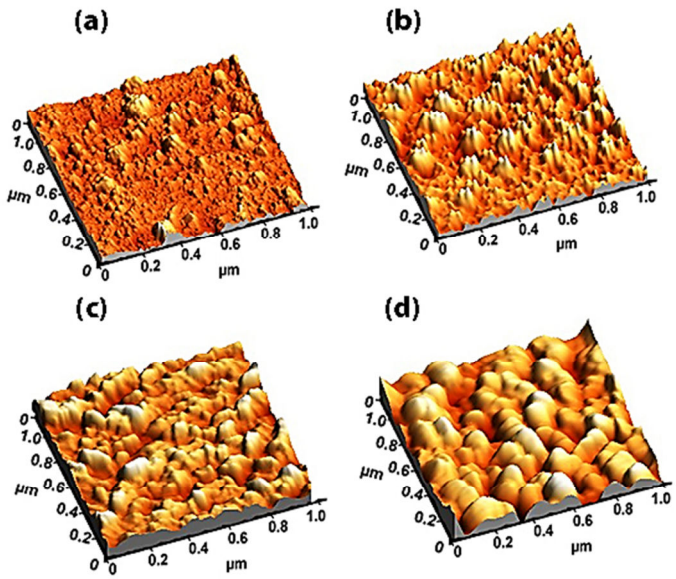

Figure 2: AFM images of nickel coated and implanted samples with different implantation energy: (a)20 keV (b) 40 keV, (c) 60 keV and (d) 80 keV.

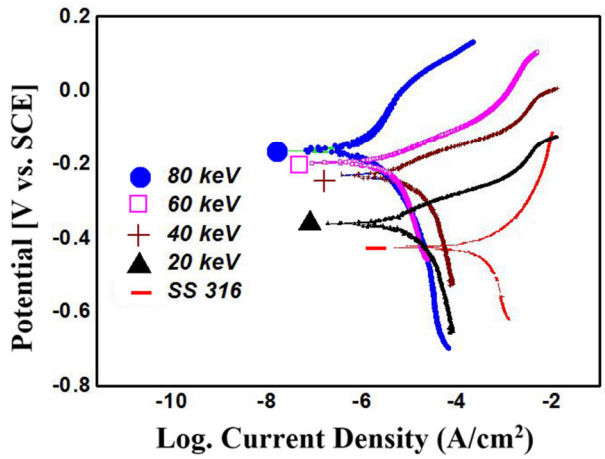

Figure 3: Polarization curves obtained for 316 SS and nickel coated and implanted samples with different implantation energy.

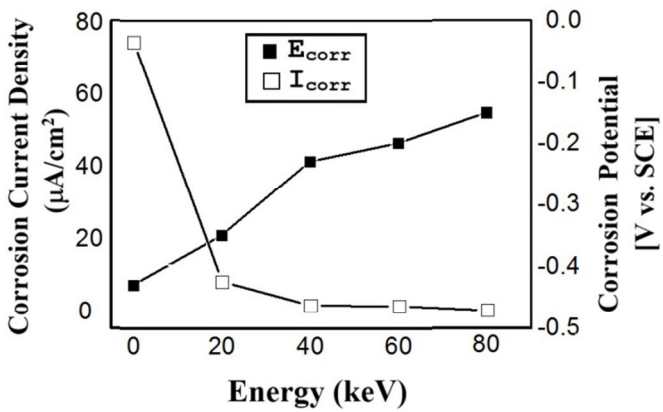

Figure 4: Corrosion current density and Corrosion potential of 316 SS and nickel coated and implanted samples with different implantation energy.

Graphical results of corrosion related parameters are given in Figure 4. From polarization and surface roughness results shown in Table 1 and the above discussion, it can be deduced that smooth surfaces provide better corrosion protection.

3.4. SEM

Figure 5 shows the SEM micrographs of N^+ ion implanted samples after corrosion test. These images are in consistent with the results obtained from polarization test (Table 1). The surface of the sample implanted at 20 keV shows large defects, like cracks and holes, indicating the corroded domains while the density of corroded domains is considerably reduced on the surface of samples obtained at other implantation energies. For the sample implanted at 80 keV, the surface is remained almost intact providing that the corrosion rate is decreased. It can also be observed that by increasing the energy of the nitrogen ions, larger domains with wider and dark corroded areas are decreased. All of the observations are in agreement with the results of potentiodynamic test; the nitrogen ion implantation increases the corrosion resistance of samples in 3.5% NaCl medium.

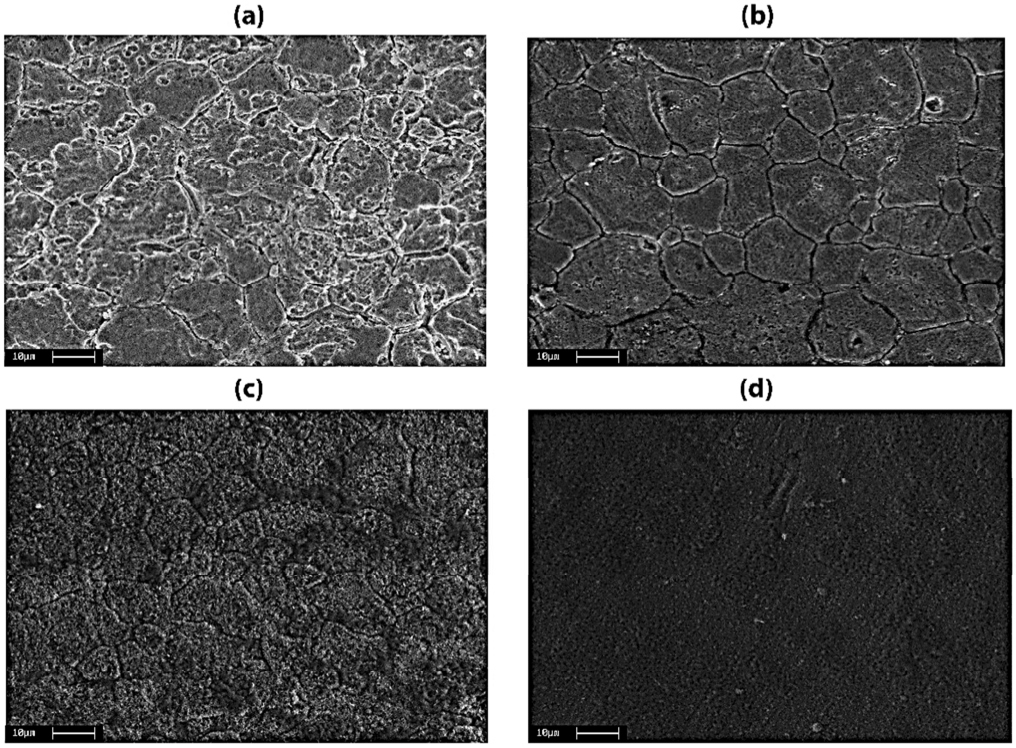

Figure 5: SEM images of nickel coated and implanted samples with different implantation energy: (a) 20 keV (b) 40 keV, (c) 60 keV and (d) 80 keV.

4. Conclusion

It has been shown that nickel coating and nitrogen implantation have dominant effect on corrosion protection. Crystallographic examination using XRD revealed the formation of nickel and nickel nitride peaks in treated samples. The nickel nitride peaks were intensified by increasing the implantation energy, while the nickel lines were weakened. After nitrogen implantation, the surface morphology study using AFM showed surface smothering with an increase in implantation energy. It was observed from polarization plots that the increase in ion energy modifies the corrosion resistance. After corrosion test, the SEM images confirmed again more protective surface for higher energies. Moreover, resistance to grain boundary attack with increase in energy values is clearly observed.

5. References

1. H. P. Feng, C. H. Hsu, J. K. Lu, Y. H. Shy, Effects of PVD sputtered coatings on the corrosion resistance of AISI 304 stainless steel, *Mat. Sci. Eng. A,* 347(2003), 123-129
2. X. B. Tian, Y. X. Leng, T. K. Kwok, L. P. Wang, B. Y. Tang, P. K. Chu, Hybrid elevated-temperature, lowrhigh-voltage plasma immersion ion implantation of AISI304 stainless steel, *Surf. Coat. Tech*., 135(2001), 178-183
3. H. Savaloni, M. Habibi, Influence of Ni deposition and subsequent N^+ ion implantation at different substrate temperatures on nano-structure and corrosion behaviour of type 316 and 304 stainless steels, *Appl. Surf. Sci.,* 258(2011), 103– 112

4. S. R. Kappaganthu, Y. Sun, Formation of an MN-type cubic nitride phase in reactively sputtered stainless steel-nitrogen films, *J. Crys. Grow*., 267(2004), 385-393.
5. R. Merello, F. J. Botana, J. Botella, M. V. Matres,M. Marcos, Influence of chemical composition on thepitting corrosion resistance of non-standardlow-Ni high-Mn–N duplex stainless steels, *Corr. Sci*., 45(2003), 909-921.
6. Y. H. Jang, S. S. Kim, J.H. Lee, Effect of different Mn contents on tensile and corrosion behavior of CD4MCU cast duplex stainless steels, *Mater. Sci. Eng. A*, 396(2005), 302-310.
7. W. Diqing, W. Jincheng, W. Gaifang, C. Xianyi, L. Linlin, F. Zhigang, Y. Gencang, Effect of Mn on damping capacities, mechanical properties, and corrosion behaviour of high damping Mg–3wt.%Ni based alloy, *Mater. Sci. Eng. A*, 494(2008), 139–142.
8. K. Park, H. Kwon, Effects of Mn on the localized corrosion behavior of Fe–18Cr alloys, *Elect. Acta*, 55(2010), 3421–3427.
9. Iu. H Toor, P. J. Hyun, H. S. Kwon, Development of high Mn–N duplex stainless steel for automobile structural components, *Corr. Sci*., 50(2008), 404–410.
10. P. Saravanan, V. S. Raja, S. Mukherjee, Effect of plasma immersion ion implantation of nitrogen on the wear and corrosion behavior of 316LVM stainless steel, *Surf. Coat. Tech*., 201(2007), 8131-8135.
11. A. R. Grayeli Korpi, Kh. M. Bahmanpour, Influence of nitrogen ion implantation on the structure and corrosion resistance of stainless steel substrates coated with Ni nanolayer, *Prog. Color Colorants Coat*., 9(2016), 77-83.
12. A. R. Grayeli Korpi, P. Balashabadi, M. M. Larijani, M. Habibi, A. Hamidi, M. Malek, Effect of gas ratio on tribological and corrosion properties of ion beam sputter deposited tin coatings, *Prog. Color Colorants Coat*., 11(2018), 129-135.
13. V. Muthupandi, P. Bala Srinivasan, V. Shankar, S. K. Seshadri, S. Sundaresan, Effect of nickel and nitrogen addition on the microstructure andmechanical properties of power beam processed duplex stainless steel (UNS 31803) weld metals, *Mater. Let.,* 59(2005), 2305-2309.
14. T. Czerwiec, N. Renevier, H. Michel, Low-temperature plasma-assisted nitriding, *Surf. Coat. Tech*., 131(2000), 267-277.
15. Y. Fu, X. Wu, E-H Han, W. Ke, K. Yang, Z. Jiang, Effects of nitrogen on the passivation of nickel-free high nitrogen and manganese stainless steels in acidic chloride solutions, *Elect. Acta*, 54(2009), 4005-4014.
16. C. Garcia, F. Martin, Y. Blanco, M.P. de Tiedra, M.L. Aparicio, Corrosion behaviour of duplex stainless steels sintered in nitrogen, *Corr. Sci*., 51(2009), 76-86.
17. F. M. Bayoumi, W. A. Ghanem, Effect of nitrogen on the corrosion behavior of austenitic stainless steel in chloride solutions, *Mater. Let*., 59(2005), 3311-3314
18. E. Poorqasemi, O. Abootalebi, M. Peikari, F. Haqdar, Investigating accuracy of the Tafel extrapolation method in HCl solutions, *Corr. Sci*., 51(2009), 1043-1054.
19. J. I. Langford, A. J. Wilson, Scherrer after sixty years: A survey and some new results in the determination of crystallite size, *J. Appl. Crys*., 11(1978), 102-113.
20. T. C. Huang, G. Lim, F. Parmigiani, E. Kay, Effect of ion bombardment during deposition on the x-ray microstructure of thin silver films, *J. Vac. Sci. Tech. A,* 3(1985), 2161-2166.
21. S. H. Ahn, J. H. Lee, J. G. Kim, J. G. Han, Localized corrosion mechanisms of the multilayered coatings related to growth defects, *Surf. Coat. Tech*., 177-178(2004), 638-644.
22. H. Klung, L. Alexander, X-Ray Diffraction Procedure, Wiley, New York, 1954, 503–524.

How to cite this article:

A. Grayeli Korpi, S. Rezaee, P. Balashabadi, Influence of Ni deposition and subsequent N^+ ion implantation at different implantation energies on nano-structure and corrosion behavior of 316 stainless steels. Prog. Color Colorants Coat., 12 (2019), 203-209.